Journal of Alloys and Compounds 509 (2011) 7004–7008

Contents lists available at ScienceDirect

Journal of Alloys and Compounds

journal homepage: www.elsevier.com/locate/jallcom

Synthesis and study of nanocrystalline Ni–Cu–Zn ferrites prepared by oxalate based precursor method

A.T. Raghavender[a,*], Sagar E. Shirsath[b], K. Vijaya Kumar[c]

[a] Nanomagnetism Lab, Department of Physics and Astronomy, Seoul National University, Seoul 151-747, South Korea
[b] Department of Physics, Vivekanand College, Aurangabad, Maharashtra 431004, India
[c] Department of Physics, Jawaharlal Nehru Technological University Hyderabad, College of Engineering, Nachupally (Kondagattu), Karimnagar-Dist., 505 501, A.P., India

ARTICLE INFO

Article history:
Received 20 January 2011
Received in revised form 16 March 2011
Accepted 19 March 2011
Available online 29 March 2011

Keywords:
Ni–Cu–Zn ferrites
Oxalate method
Nanocrystalline
Structural
Electrical
Magnetic properties

ABSTRACT

Nanocrystalline ferrites of compositions $Ni_{0.5+1.5x}Cu_{0.3}Zn_{0.2}Fe_{2-x}O_4$ ($0 \le x \le 0.5$) have been synthesized by using oxalate based precursor method at very low temperature. The Ni–Cu–Zn ferrite powder particles were obtained at 450 °C and they exhibit a crystallite size of 16–24 nm. The lattice constants were found nearly equal in all these samples due to minute difference in the ionic radius between Ni^{2+} and Fe^{3+} ions. The thermal analysis has showed the ferrite phase formation at very low temperature 377 °C. The two main spectroscopic bands corresponding to lattice vibrations were observed in the wavelength range from 300 to 1000 cm^{-1}. The IR bands at 570 cm^{-1} (ν_1) and 390 cm^{-1} (ν_2) were assigned to tetrahedral (A) and octahedral [B] groups. The spectroscopic bands shift with the increase of doping concentration. The magnetization was found to decrease with increasing doping concentration. The dielectric constant (ε') and dielectric loss tangent ($\tan\delta$) decreased with increase of frequency. The dielectric constant and dielectric loss obtained for the nanocrystalline ferrite samples appeared to be lower than that of the ferrites prepared by other synthesis techniques.

© 2011 Elsevier B.V. All rights reserved.

1. Introduction

Ferrites are essential materials in several electronic devices such as televisions, gyrators, and antennas. Though the ferrites are known as old magnetic materials which are been studied from decades still the material physicists and engineers are investigating their properties by substituting with divalent, trivalent, rare-earth materials, etc. by using different synthesis techniques. Since two decades after the emergence of nanotechnology, ferrites are being realized in nanosize using new synthesis techniques which showed novel structural, electrical and magnetic properties compared to their bulk counter parts [1]. These properties primarily depend on the preparation conditions such as synthesis techniques, heat treatment, type of substitution, etc.

Ferrites (AFe_2O_4, A = Ni, Cu, Zn, Mn, Co) have high potential for many new technological applications, e.g. magnetic recording media and storage, MRI enhancement, magnetically guided drug delivery, and wastewater treatment. Spinel zinc ferrite ($ZnFe_2O_4$) is paramagnetic and exhibits antiferromagnetism with the Neel temperature (T_N) of about 10 K [2]. On the other hand, nickel ferrite ($NiFe_2O_4$) has an inverse spinel structure showing ferrimagnetism that originates from magnetic moment of anti-parrallel spins between Fe^{3+} ions at tetrahedral sites and Ni^{2+} ions at octahedral sites [3]. It was suggested recently that Ni, Cu and Zn ferrites offer superior magnetic properties depending on certain concentration of Ni, Cu, Zn in the ferrites [4]. In order to develop multilayer chip inductor the Ni–Zn–Cu ferrites were intensively studied in the last 10 years [5]. Ni–Cu–Zn ferrites are well established soft magnetic material for multilayer chip inductors (MLCs) applications because of their relatively low sintering temperature, high permeability in the RF frequency region and high electrical resistivity [6–9]. The magnetic properties of the ferrites are highly sensitive to the technology parameters, especially to the amount of constituent metal ions or additives in their compositions [10]. The magnetic properties can be changed by the substitution of various kinds of M^{2+} divalent cations (Co^{2+}, Mg^{2+}, Fe^{2+}, Mn^{2+}) or by introducing a relatively small amount of rare-earth ions [11].

Synthesis of nanoferrites using oxalates is gaining a lot of interest at present. Oxalate based precursor method is a simple synthesis technique and can be adapted for preparing complex samples. The oxalates synthesis method was suggested by Wickham [12] and subsequently modified by Bremer et al. [13] for synthesis of Mn–Zn ferrites. The oxalate precursor for synthesis of ferrite has been widely employed and found convenient, since it yields a homogeneous product in short time [14,15]. Oxalates are generally preferred because of their low solubility; low decomposition temperature and fine particle yield [16]. Their prime advantage is in achieving intimate mixing on an atomic scale resulting in the

* Corresponding author. Tel.: +82 2 880 6606; fax: +82 2 884 3002.
E-mail address: atraghavender@snu.ac.kr (A.T. Raghavender).

0925-8388/$ – see front matter © 2011 Elsevier B.V. All rights reserved.
doi:10.1016/j.jallcom.2011.03.127

formation of true solid solution [17]. This uniformity in starting materials favours the diffusion dependent formation of homogeneous spinel at low temperature.

Since, no reports have been sighted in the literature on the synthesis of nanocrystalline $Ni_{0.5+1.5x}Cu_{0.3}Zn_{0.2}Fe_{2-x}O_4$ ($0 \le x \le 0.5$) by oxalate based precursor method, in this present study we aimed at the synthesis of Ni–Cu–Zn ferrites. We report and discussed the low temperature synthesis of Ni–Cu–Zn ferrites and its crystal structure, morphology, thermal analysis, magnetic and electrical properties.

2. Experimental procedure

Nanocrystalline Ni^{2+} substituted Cu–Zn ferrite with a generic formula $Ni_{0.5+1.5x}Cu_{0.3}Zn_{0.2}Fe_{2-x}O_4$ ($0 \le x \le 0.5$) were synthesized by oxalate based precursor method [12–17]. All of the chemicals were analytical grade from Sigma–Aldrich with purity ≥99% and were used without any further purification. In a typical procedure, the nickel nitrate hydrate $Ni(NO_3)_2{\cdot}6H_2O$, cupric nitrate hydrate $Cu(NO_3)_2{\cdot}6H_2O$, zinc nitrate hydrate $Zn(NO_3)_2{\cdot}6H_2O$, ferric nitrate nonahydrate $Fe(NO_3)_3{\cdot}9H_2O$ were used as starting materials. Stoichiometric amounts of metal nitrates were dissolved in deionized water to get clear solution. The obtained aqueous solution of metal nitrates was mixed with oxalic acid in a molar ratio ranging from 1:3 to 1:0.15. The mixture solution were moved on to magnetic stirrer and stirred for 2 h at room temperature. The reaction mixtures turned turbid by varying molar ratios 1:3 and 1:2. When the molar ratio was further lowered to 1:1, precursor solution showed different colour shades. The resultant mixtures were evaporated on a hot plate at ~150 °C for 2 h. The obtained raw powders were thermally heat treated at 450 °C for 4 h.

Structural characterization of the obtained ferrite powders was carried out on Inel X-ray diffraction (XRD) system with Ni filter using Co Kα radiation (wavelength, λ = 1.78894 Å). The average particle size (D) was calculated using most intense peak (3 1 1) employing the Scherrer formula. Thermogravimetric (TG) and differential thermal analysis (DTA) of the dried powder of Ni–Cu–Zn ferrite was carried using Netzsch STA 409 TG–DTA instrument, at a heating rate of 10 °C/min in static air. Transmission IR spectra in the range 300–1000 cm^{-1} were recorded using a FTIR (Perkin Elmer FT-IR Spectrometer). The samples were mixed with spectral grade KBr (Potassium Bromide) as the standard. TEM studies were carried out using Philips CM-12 transmission electron microscope (TEM). Magnetic measurements were performed using the vibrating sample magnetometer VSM 4500. Dielectric measurements were carried out at room temperature using a 4192A impedance analyzer.

3. Results and discussions

Fig. 1 shows the X-ray diffraction patterns of $Ni_{0.5+1.5x}Cu_{0.3}Zn_{0.2}Fe_{2-x}O_4$ ($0 \le x \le 0.5$) nanocrystallites. XRD patterns reveal that the prepared samples are single phase. The crystallite size were evaluated by measuring the full width half maximum (FWHM) of the most intense peak (3 1 1). The results are as shown in Table 1. The crystallite size was observed in the range of 16–24 nm. The values for lattice constants were obtained for all the samples using XRD data with an accuracy of ±0.002 Å and are listed in Table 1. It clearly shows that the lattice constants are nearly equal for all the samples. This behaviour of lattice constant can be explained on the basis of small difference in ionic radii of Ni^{2+} and Fe^{3+}. In the present series $Ni_{0.5+1.5x}Cu_{0.3}Zn_{0.2}Fe_{2-x}O_4$, the ionic radius of Ni^{2+} (0.69 Å) and Fe^{3+} (0.67 Å) are found to be very similar, due to this small difference in ionic radii the lattice constants seem to be not largely affected. Similar trend was found in $Ni_{0.7-x}Cu_xZn_{0.3}Fe_2O_4$ ferrite synthesized using egg-white [18].

Table 1
Dependence of particle size d, lattice constant a, IR frequency ν_1, ν_2 and magnetization M on $Ni_{0.5+1.5x}Cu_{0.3}Zn_{0.2}Fe_{2-x}O_4$ ($0 \le x \le 0.5$).

x	d (nm)	a (Å)	ν_1 (cm^{-1})	ν_2 (cm^{-1})	M (emu/g)
0.0	16	8.329	549	389	56.1
0.1	21	8.351	570	393	55.6
0.2	19	8.344	569	395	51.8
0.3	22	8.349	555	391	48.5
0.4	21	8.355	568	393	46.9
0.5	24	8.356	569	393	43.1

Thermal analysis for the sample $x = 0.0$ was carried out in the temperature range of 200–500 °C in static air at 10 °C/min. Fig. 2 shows TG–DTA for $Ni_{0.5}Cu_{0.3}Zn_{0.2}Fe_2O_4$ powder and it shows the presence of one exothermic peak at 377 °C which may be due to the reaction of oxalates and metal nitrates, with total weight loss around 7%. Further, no weight changes were observed below this temperature. Thus the ferrite phase formation has taken place at very low temperature 377 °C. It may be mentioned that the formation of the spinel phase is at a temperature lower than 377 °C while thermal analysis is a dynamic process. Thus, the temperature recorded by TG–DTA for spinel formation is expected to be higher. It is observed from acetate-citrate gelation method [19] that above 430 °C, only the organics are removed completely, and the prediction of particle size and further analysis is irrelevant below this temperature. Therefore, even though the decomposition has completed at 377 °C, we have chosen 450 °C as final calcination temperature for all the samples. The preparation of ferrites around this temperature was confirmed by XRD data.

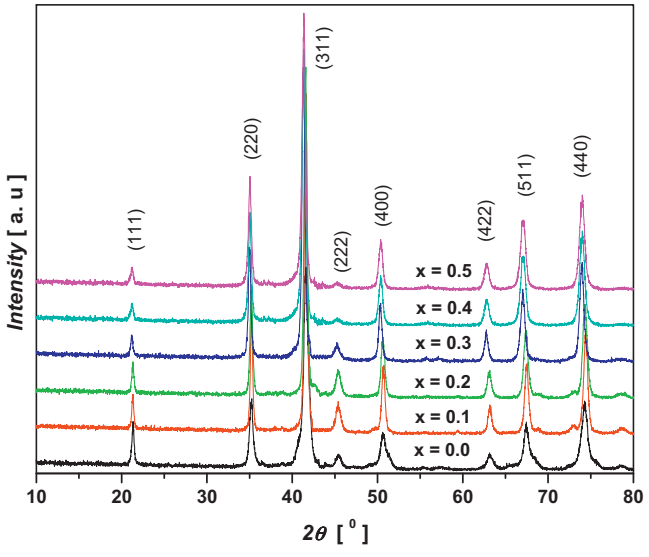

Fig. 1. X-ray diffraction pattern of $Ni_{0.5+1.5x}Cu_{0.3}Zn_{0.2}Fe_{2-x}O_4$ ($0 \le x \le 0.5$) nanoparticles.

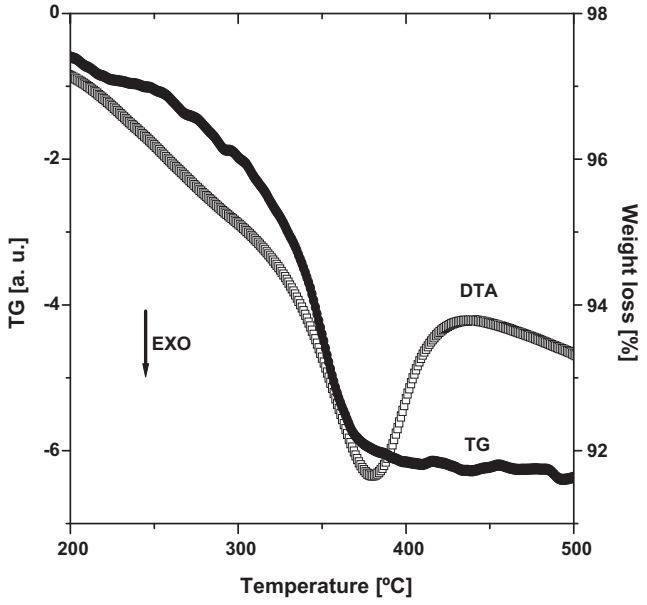

Fig. 2. TG–DTA of $Ni_{0.5}Cu_{0.3}Zn_{0.2}Fe_2O_4$.

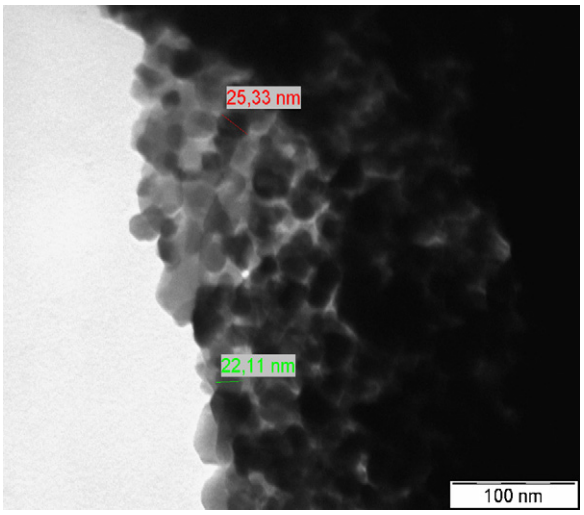

Fig. 3. TEM image $Ni_{0.5}Cu_{0.3}Zn_{0.2}Fe_2O_4$.

Fig. 3 shows the TEM image for the composition $x = 0.0$. TEM image clearly show that the synthesized ferrites are nanocrystallites. The observed crystallite sizes are in the range of 16–25 nm. The crystallite sizes measured from XRD are very well in agreement with the TEM images.

Infrared spectra of all the samples were recorded in order to confirm the ferrite formation and to support the XRD data. The IR spectra of $Ni_{0.5+1.5x}Cu_{0.3}Zn_{0.2}Fe_{2-x}O_4$ ($0 \le x \le 0.5$) are presented in Fig. 4. $Ni_{0.5+1.5x}Cu_{0.3}Zn_{0.2}Fe_{2-x}O_4$ gives rise to two main absorption envelopes, consisting of metal–oxygen stretching bands ν_1 and ν_2, in the range 600–560 and 400–380 cm^{-1}, respectively. The ν_1 band corresponds to intrinsic stretching vibrations of tetrahedral Fe^{3+}–O, while ν_2 is assigned to Fe^{3+}–O and M–O (where M = Ni, Cu, Zn) bond stretching vibrations of octahedral sites [20,21]. The corresponding values of IR are as presented in Table 1. From Fig. 4 it can be seen that the IR spectra consist of bands corresponding to tetrahedral and octahedral bonds only. The band position shifts slightly with the increase in doping concentration. It is well known from

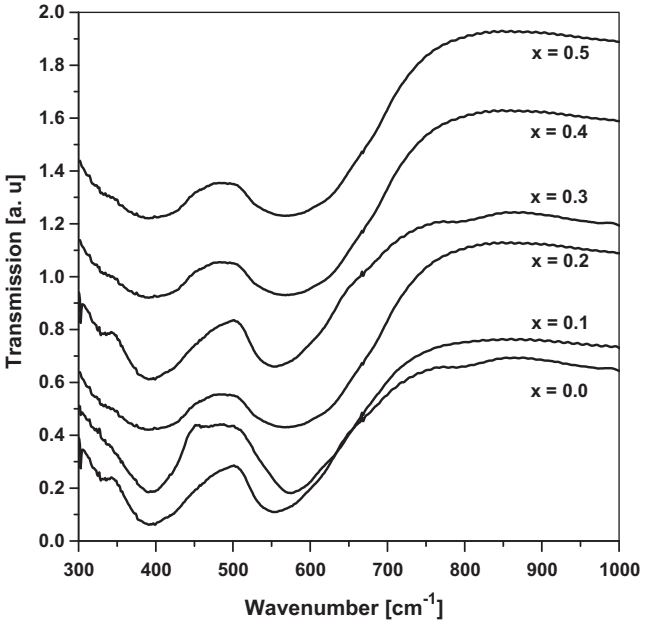

Fig. 4. Infrared spectra in the 1000–300 cm^{-1} range for nanocrystalline $Ni_{0.5+1.5x}Cu_{0.3}Zn_{0.2}Fe_{2-x}O_4$ ($0 \le x \le 0.5$).

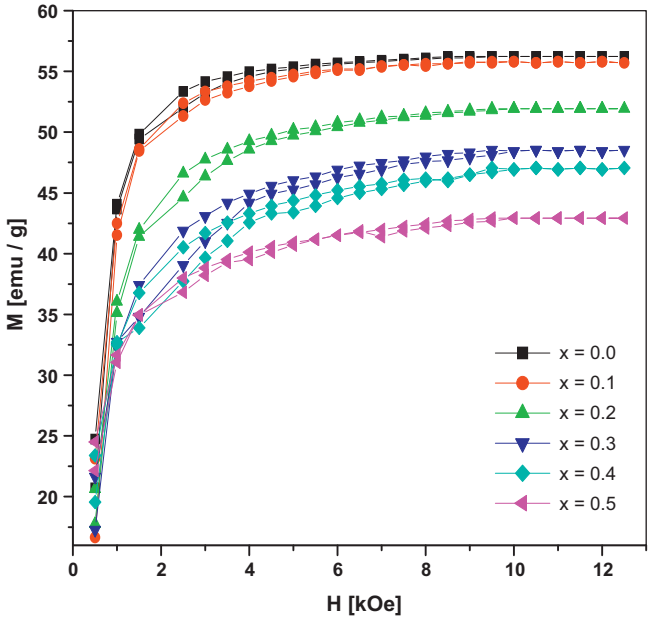

Fig. 5. Variation of magnetization M (emu/g) with H (kOe) for $Ni_{0.5+1.5x}Cu_{0.3}Zn_{0.2}Fe_{2-x}O_4$ ($0 \le x \le 0.5$).

literature [18,22,23] that Ni^{2+} and Cu^{2+} ions prefer octahedral sites where as Zn^{2+} ions prefer tetrahedral sites and Fe^{3+} being distributed between octahedral and tetrahedral sites. Therefore, the cation distribution can be assumed as $(Zn_{0.2}Fe_{0.8})^A[Ni_{0.5+1.5x}Cu_{0.3}Fe_{1.2}]^B$ respectively. So from IR band positions (Table 1) and from the cation distribution one can assume the change in band positions with doping concentration x. Taking these features into consideration, it is evident from the measured IR spectra that single phase ferrites have been synthesized. In the other words, infrared spectra undoubtedly support the XRD data.

Magnetization measurements of nanocrystalline $Ni_{0.5+1.5x}Cu_{0.3}Zn_{0.2}Fe_{2-x}O_4$ ($0 \le x \le 0.5$) were carried out using vibrating sample magnetometer with maximum applied field of 12.5 kOe at room temperature. The obtained magnetic curves are shown in Fig. 5. All the samples show the ferromagnetic nature. The maximum magnetization values (M) obtained from the magnetic data are presented in Table 1. The magnetization was found to decrease with increasing doping concentration. In ferrites, the magnetic moment arises mainly from the parallel uncompensated electron spin of the individual ions. The intensity of magnetization thus can be explained by considering the cation distribution and antiparallel spin alignment of the two sublattices as given by Néel model [24]. Since the Zn^{2+} ions are non-magnetic, the magnetization will be mainly de to Ni^{2+}, Cu^{2+} and Fe^{3+} ions having magnetic moment of 2.3, 1.3 and 5 μ_B, respectively. In the present case Ni^{2+} ions of magnetic moment 2.3 μ_B replaces Fe^{3+} ions of magnetic moment 5 μ_B. Accordingly, the net magnetization is expected to decrease with increasing Ni^{2+}. The gradual decrease in the magnetization with increasing Ni^{2+} content x may be accounted for the weakening of A–B interaction, similar kind of trend was observed for Al substituted Ni–Cu–Zn Ferrite [18].

Fig. 6 shows the variation of dielectric constant with frequency for all the samples. It can be seen from Fig. 6 that the dielectric constant (ε') decreases with the increase in frequency. As more dielectric dispersion is observed at low frequency region, this observed behaviour may be due to the Maxwell–Wagner interfacial type of polarization [25,26], which is in agreement with Koops phenomenological theory [27]. The decrease of polarization with increase of frequency is due to the fact that, beyond a certain fre-

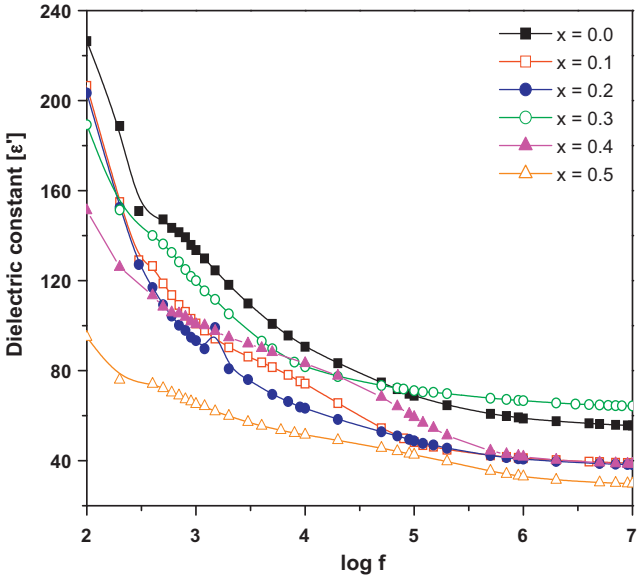

Fig. 6. Variation in dielectric constant (ε') with frequency ($\log f$).

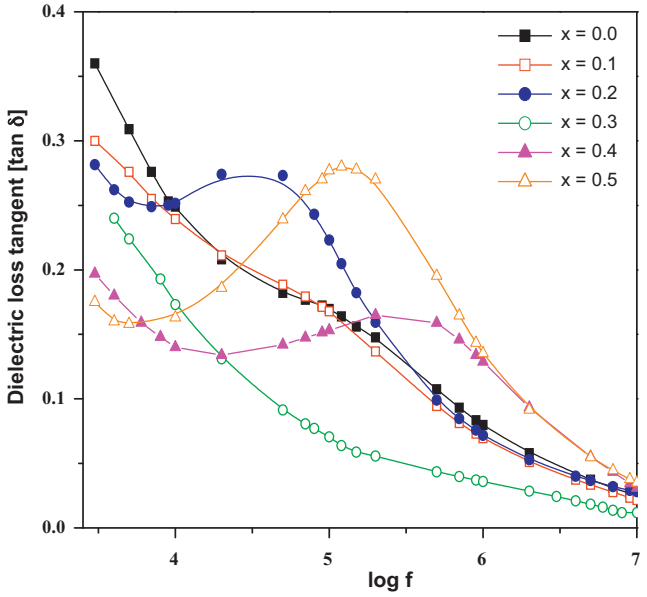

Fig. 8. Variation in dielectric loss tangent ($\tan\delta$) with frequency ($\log f$).

quency of the electric field, the electronic exchange between Fe^{2+} and Fe^{3+} cannot follow the alternating field, therefore the real part of dielectric constant (ε') decrease with increasing frequency. In the present series of $Ni_{0.5+1.5x}Cu_{0.3}Zn_{0.2}Fe_{2-x}O_4$ the preference of Ni^{2+} ions at octahedral [B] site, Fe^{3+} ions on tetrahedral (A) site and octahedral [B] site favours the following exchange interaction:

$$Ni^{2+} + Fe^{3+} \leftrightarrow Ni^{3+} + Fe^{2+}$$

Thus, the conduction mechanism for the n-type semiconductor is predominantly due to the hopping of electrons from Fe^{2+} to Fe^{3+} while that for the p-type semiconductor is due to the transfer from Ni^{3+} to Ni^{2+} [28]. According to Rabkin and Novikova [29], the process of dielectric polarization in ferrites takes place through a mechanism similar to conduction process by electron exchange between $Fe^{2+} \leftrightarrow Fe^{3+}$ and $Ni^{2+} \leftrightarrow Ni^{3+}$ from which one obtains local displacement of the electrons in the direction of electrical field; these displacements determines the polarization.

A plot of variation of dielectric constant with Ni^{2+} content x is shown in Fig. 7. It is clear that ε' decreases with increasing Ni^{2+} content. This may indicate the possibility of decrease of hopping interaction with increasing addition of Ni^{2+}. Further, in Ni–Cu–Zn ferrites, zinc ions occupy tetrahedral (A) sites whereas Ni ions prefer to go to octahedral [B] sites. Fe ions which exist in 2+ as well as in 3+ states, occupy both A- and B-sites. The Fe^{3+} concentration at the octahedral sites is maximal for the sample with the compositional variable $x = 0.0$. The number of Fe^{2+} ions on the octahedral sites that take part in the electron exchange interaction $Fe^{2+} \leftrightarrow Fe^{3+}$, and hence are responsible for the polarisation, is maximal for $x = 0.0$; therefore, a comparatively high value of the dielectric constant is expected. The substitution of Ni^{2+} ions alters the iron ion concentration from the initial composition in each substitution stage, thereby decreasing the number of ferrous ions on the octahedral sites that are available for polarization and consequently decreasing the dielectric constant. Ni^{2+} ions present at B sites localize Fe^{2+} ions by forming stable electronic bonds with Fe^{2+} ions. This localization effect obstructs the electron exchange interaction $Fe^{2+} \leftrightarrow Fe^{3+}$ by reducing the effective number of free Fe^{2+} ions, which consequently decreases the dielectric constant. This is due to the decrease in the number of ferrous ions on the octahedral sites. This result agrees with the assumption made by Rabinkin and Novikova [29].

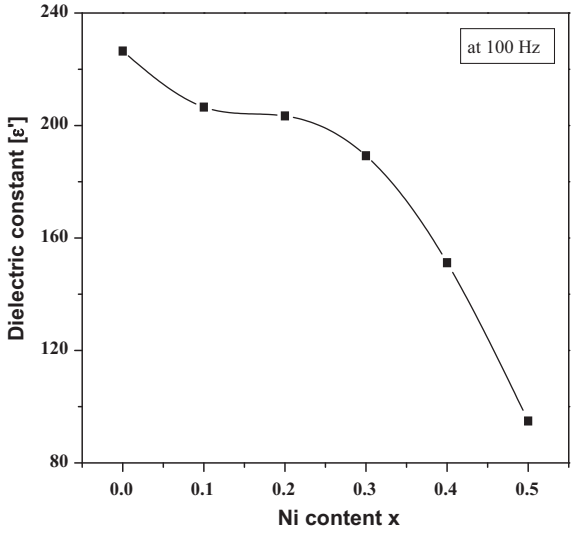

Fig. 7. Variation in dielectric constant (ε') with Ni content x.

The variation of dielectric loss tangent ($\tan\delta$) against logarithm of frequency ($\log f$) for various compositions are shown in Fig. 8. All the compositions show normal dielectric behaviour. It is observed from Fig. 8 that the dielectric loss tangent decreases exponentially with increase in frequency for all the samples under investigation. A maxima in dielectric loss tangent versus frequency appears when frequency of the hopping charge carriers coincides with frequency of the applied alternating field. The maxima in dielectric loss tangent decreases with increase in frequency and broad peak disappears for higher frequency. A broad peak of dielectric loss tangent indicates existence of a distribution of relaxation time rather than a single relaxation time [30]. The condition for observing maxima in dielectric loss tangent of a material is $\omega\tau = 1$ where $\omega = 2\pi f_{max}$ and τ is relaxation time. Now, the relaxation time is related to jumping probability per unit time P by relation

$$\tau = \frac{1}{2}P \quad \text{or} \quad f_{max} \propto P.$$

4. Conclusions

Nanocrystalline $Ni_{0.5+1.5x}Cu_{0.3}Zn_{0.2}Fe_{2-x}O_4$ ($0 \le x \le 0.5$) ferrites were synthesized by using oxalate based precursor method at very low temperature and with particle size from 16 to 24 nm. The lattice constants were found to be nearly equal. The study of thermal analysis of all the ferrites indicate the formation of spinel phase at 377 °C. The IR analysis of all the ferrites revealed the existence of high frequency metal–oxygen bands corresponding to intrinsic stretching vibrations of tetrahedral and octahedral sites. The magnetization was found to decrease with increasing doping concentration. The dielectric constant and dielectric loss tangent decreased with increase in frequency. The low dielectric behaviour makes ferrite materials useful in high frequency applications.

Acknowledgements

The author, ATR, thanks "BK21 Frontier Physics Research Division, Department of Physics and Astronomy, Seoul National University, Seoul, South Korea" for the Postdoctoral Fellowship. The author KVK expressed his gratitude to Dr. A. Govardhan, Principal, JNTUH College of Engineering, Nachupally (Kondagattu), Karimnagar-Dist., A.P., India for his cooperation.

References

[1] M. Hosokawa, K. Nogi, M. Naito, T. Yokoyama, Nanoparticle Technology Handbook, Elsevier, The Netherlands, 2007.
[2] K. Kamazawa, Y. Tsunoda, K. Odaka, K. Kohn, J. Phys. Chem. Solids 60 (1999) 261.
[3] Y. Kinemuchi, K. Ishizaka, H. Suematsu, W. Jiang, K. Yatsui, Thin Solid Films 407 (2002) 109.
[4] S. Maensiri, C. Masingboon, B. Boonchom, S. Seraphin, Scr. Mater. 56 (2007) 797.
[5] S.F. Wang, Y.R. Wang, T.C.K. Yang, C.F. Chen, C.A. Lu, C.Y. Huang, J. Magn. Magn. Mater. 220 (2000) 129.
[6] K.O. Low, F.R. Sale, J. Magn. Magn. Mater. 246 (2002) 30.
[7] H.I. Hsiang, W.C. Liao, Y.J. Wang, Y.F. Cheng, J. Eur. Ceram. Soc. 24 (2004) 2015.
[8] Y.P. Fu, J. Am. Ceram. Soc. 89 (2006) 3547.
[9] Z. Yue, L. Li, J. Zhou, H. Zhang, Z. Ma, Z. Gui, Mater. Lett. 44 (2000) 279.
[10] O.F. Caltum, L. Spinu, Al. Stancu, L.D. Thung, W. Zhou, J. Magn. Magn. Mater. 242–245 (2002) 160.
[11] L. Zhao, Y. Cui, H. Yang, L. Yu, W. Jin, S. Feng, Mater. Lett. 60 (2006) 104–108.
[12] D.G. Wickham, Inorg. Synth. 9 (1967) 152.
[13] M. Bremer, St. Fisher, H. Langbein, W. Topelmann, H. Scheler, Thermochim. Acta 209 (1992) 323.
[14] D.N. Bhosale, N.D. Chaudhari, S.R. Sawant, P.P. Bakare, J. Magn. Magn. Mater. 173 (1997) 51.
[15] N.D. Chaudhari, R.C. Kambale, J.Y. Patil, S.R. Sawant, S.S. Suryavanshi, Mater. Res. Bull. 45 (2010) 1713.
[16] M. Paulus, in: P. Hagnemular (Ed.), Preparative Methods in Solid State Chemistry, Academic Press, NY, 1972, p. 487.
[17] K.C. Patil, S. Sundermanmohan, D. Gajapthy, in: N.P. Cheremisinoff (Ed.), Handbook of Ceramics and Composites, vol. 1, Marcel Dekkar, NY, 1990, p. 469.
[18] M.A. Gabal, Y.M. Al Angari, S.S. Al-Juaid, J. Alloys Compd. 492 (2010) 411.
[19] D. Mondelaers, G. Vanhoyland, H. Van den Rul, J. D'Haen, M.K. Van Bael, J. Mullens, L.C. Van Poucke, Mater. Res. Bull. 37 (2002) 901.
[20] R.D. Waldron, Phys. Rev. 99 (1955) 1727.
[21] F.A. Cotton, G. Wilkinson, Advanced Inorganic Chemistry, 5th ed., John Willey & Sons, New York, 1988, p. 9.
[22] L.J. Ma, L.S. Chen, S.Y. Chen, Mater. Chem. Phys. 114 (2009) 692.
[23] A.T. Raghavender, N. Biliškov, Ž. Skoko, Mater. Lett. 65 (2011) 677.
[24] Y.P. Fu, S. Tsao, C.T. Hu, Y.D. Yao, J. Alloys Compd. 395 (2005) 272.
[25] J.C. Maxwell, Electricity and Magnetism, vol. 1, Oxford University Press, London, 1873, Sec. 328.
[26] K.W. Wagner, Ann. Phys. (Leipzig) 40 (1913) 817.
[27] C.G. Koops, Phys. Rev. 83 (1951) 121.
[28] L.G. Van Uitert, J. Chem. Phys. 23 (1955) 1883.
[29] R.I. Rabkin, Z.I. Novikova, Ferotes, Izs, Acad. Nauk, BSSR Minsk (1960) 146.
[30] T. Murase, K. Igarahi, J. Sawai, Nomura, ICF 7,B3, Bordeaux (France), 1996.